A New Class of Lasing Materials: Intrinsic Stimulated Emission from Nonlinear Optically Active Metal-Organic Frameworks

Medishetty, Raghavender; Nalla, Venkatram; Nemec, Lydia; Henke, Sebastian; Mayer, David; Sun, Handong; Reuter, Karsten; Fischer, Roland A.

2017

Medishetty, R., Nalla, V., Nemec, L., Henke, S., Mayer, D., Sun, H., et al. (2017). A New Class of Lasing Materials: Intrinsic Stimulated Emission from Nonlinear Optically Active Metal-Organic Frameworks. Advanced Materials, in press.

https://hdl.handle.net/10356/80237

https://doi.org/10.1002/adma.201605637

A New Class of Lasing Materials:

Intrinsic Stimulated Emission from Nonlinear Optical Active Metal-Organic Frameworks

Raghavender Medishetty[1], Venkatram Nalla[2]*, Sebastian Henke[3], Lydia Nemec[4], Handong Sun[2], Karsten Reuter[4]*, Roland A. Fischer[1]*

Solid state optical materials with strong nonlinear optical (NLO) and stimulated emission (STE) performance are of great interest for various photonic and sensing applications. Hybrid dielectric materials such as metal-organic frameworks (MOFs) are ideal candidates to overcome prevailing challenges to design and obtain such materials. They combine unique fluorescent mechanisms with modular versatility and control over the 3-dimensional (3D) structure through the organization of their building units in form of metal nodes and organic linkers. Two new anionic interpenetrated 3D-MOFs constructed from a tetraphenylethylene (TPE) chromophore-based linker and In(III) or Zn(II) metal ions as the nodes have been specifically designed and synthesized. These two MOFs display very strong, low threshold STE along with exceptional NLO absorption cross sections as an intrinsic property. The superior STE of Zn-MOF as compared to In-MOF is assigned to a more dense packing. Similarly, the NLO properties of these MOFs depend on the local packing arrangement and organization of the organic linkers due to the facile coupling of quadrupole moments in 3D space. Thus, loss of long-range order does not at all change the optical properties as demonstrated by the non-crystalline version of In-MOF. Moreover, the optical and thermal stability suggest these materials as potential candidates for practical applications and also represent a step-stone for designing new high performance optical materials.

[1] Chair of Inorganic and Metal-Organic Chemistry, Technical University Munich, Lichtenbergstraße 4, D-85748 Garching (Germany). [2] Centre for Disruptive Photonic Technologies, School of Physical and Mathematical Sciences, Nanyang Technological University, Singapore 637371, Singapore. [3] Chair of Inorganic Chemistry II, Organometallics and Materials Chemistry, Ruhr University Bochum, Universitätsstrasse 150, 44801 Bochum, Germany. [4] Chair of Theoretical Chemistry, Technical University Munich, Lichtenbergstraße 4, D-85748 Garching, Germany. *email: karsten.reuter@ch.tum.de; VNalla@ntu.edu.sg; roland.fischer@tum.de

Nonlinear optics (NLO), stimulated emission (STE) and lasing are fundamental aspects for the fabrication of optical photonic devices, preferably out of compact and robust solid-state materials.[1-6] Stimulated emission and its enhancement in particular is an important characteristic to produce low-threshold lasers with variable wavelengths for use as the optical gain material for applications in materials and bio-medical sciences. This property has been observed in various organic dyes, semi-conducting materials, colloidal quantum dots and polymers.[7-9] Targeting a solidification for improved practical applicability, there have been studies on the loading of such dye molecules and nanomaterials in porous metal-oxides cavities or polymer matrices. However, the NLO efficiencies and quantum yields of these composites are very limited due to several quenching mechanisms, in addition to the low loading levels.[10-13] Moreover, there have been several other drawbacks, such as poor stability or toxic behaviour in case of non-oxide materials, which limits the value of these materials in various applications.[14-16]

Solid state hybrid materials such as metal-organic frameworks (MOFs) containing aggregation induced emission (AIE) dyes as building units have shown exceptional optical behaviours.[17-19] Although the dye molecules are densely packed in these materials, the bridging of organic linkers between the metal-nodes in a rigidified and restrictive conformation can help to avoid the aggregation caused quenching and other non-radiative decay mechanisms, as well as to enhance the radiative decay of excited molecules.[18-20] Thus, MOFs appear to be the ideal candidates to produce remarkable and unprecedented optical properties towards the application in compact solid state devices.

Although there have been several reports on luminescent MOFs,[21-23] until now STE and lasing from MOFs, or coordination networks in general, as an inherent property has not been observed.[24-26] Nevertheless, by suitable choice of metal-nodes and organic linkers, properties such as colour, fluorescence decay, relaxation time and quantum yield can be designed and the respective materials can be conveniently produced, which is not possible in a similar fashion with any other system. The thermal and optical stability, long-term reliability, non-toxic/environmental friendly behaviour, robustness, economical synthesis and versatility then suggests MOFs as a class of materials with great promise for novel optical gain media to produce low threshold lasers.

In this work, we report on the design and function of two 3D MOFs which are derived from tetrakis[4-(4-carboxyphenyl)phenyl]ethene (H_4TCPE) linkers coordinated with In(III) and Zn(II) nodes through carboxylates. These materials show an exceptional two-photon excited fluorescence (2PEF) and stimulated emission (STE). The 2PEF action cross section values are estimated as 3072 GM and 1053 GM for In- and Zn-MOF respectively at 650 nm, which is much higher than those of many organic commercial dye molecules, polymers and nanoparticles both in solution and solid state.[27-29] Low-threshold stimulated emission is observed for the first time upon excitation of the MOFs with a 400 nm laser, as is confirmed by the appearance of a sharp peak with FWHM 18±2 nm at 470 nm for In-MOF (E_{th} = 36 mJ·cm^{-2}) and a sharp peak with

FWHM 19±1 nm at 462 nm for Zn-MOF (E_{th} = 27 mJ·cm^{-2}). In contrast, the loading of various dye molecules (DSMP) in the framework resulted in the non-radiative decay of fluorescence from the material (1PEF and 2PEF) and no stimulated emission behaviour.

Yellow coloured block shaped single crystals of (DMA)[In(TCPE)](*solv*) (In-MOF; DMA = dimethylammonium cation; *solv* = DMF and water) were obtained by solvothermal reaction between $InCl_3$ and H_4TCPE in DMF at 80 °C for 48h. This compound crystallises in the monoclinic space group *C*2/*c* and the crystal structure was determined via single crystal X-ray diffraction. The In(III) ions are coordinated pseudo-tetrahedrally by four carboxylate groups of TCPE resulting in a 3D-double interpenetrated anionic framework, with threefold disordered DMA cations in the framework pores for charge balance. The DMA cations are formed *in situ* by decomposition and protonation of the solvent DMF. The solvent accessible void space of the framework was determined to be approximately 55% (see Supporting Information, SI). From a topological and connectivity view point, the In-centres act as four connecting nodes while the TCPE linker can be regarded as bi-tri-connecting nodes, on which basis topological analysis yields a rare **tfi** net with Schläfli point symbol $(6^2{\cdot}8^4)(6^2{\cdot}8)_2$ with stoichiometry $(3\text{-c})_2(4\text{-c})$. If TCPE is further simplified as a four connecting node, the connectivity of the framework corresponds to a more simple **pts** net with stoichiometry (4-c)(4-c) with point symbol $(4^2{\cdot}8^4)$. See Fig. S4 in the supporting information (SI) for details.[30, 31]

Phase purity of the sample was confirmed by powder X-ray diffraction (PXRD) and the compound is stable up to 400 °C as evaluated by thermogravimetric analysis (TGA). Although the crystalline ordering of In-MOF is stable at ambient conditions for several days, upon activation under dynamic vacuum the material lost its long-range ordering as confirmed by PXRD. Interestingly, this less crystalline or even amorphous sample neither showed any significant change in thermal stability (as evidenced by TGA) nor changes of the photo-physical and optical behaviour. Importantly, the framework connectivity and short-range ordering persists in the material, as confirmed by the IR data of the as-synthesized and activated material (Fig. S16 in SI).[32-35] Remarkably, there is also no change in morphology and transparency of the "single crystal" even if this specimen has lost crystallinity as seen by XRD. Similar loss of crystallinity but not framework topology/connectivity (order/disorder phenomena) upon solvent loss in MOFs has been reported before and in most cases such behaviour was considered as potential disadvantage. However in the case of the discussed optical properties the effects caused by the loss of long-range order of the coordination network seem insignificant. This observation may open up the opportunity to think beyond crystallinity in MOFs/coordination networks for optical functions.[32-35]

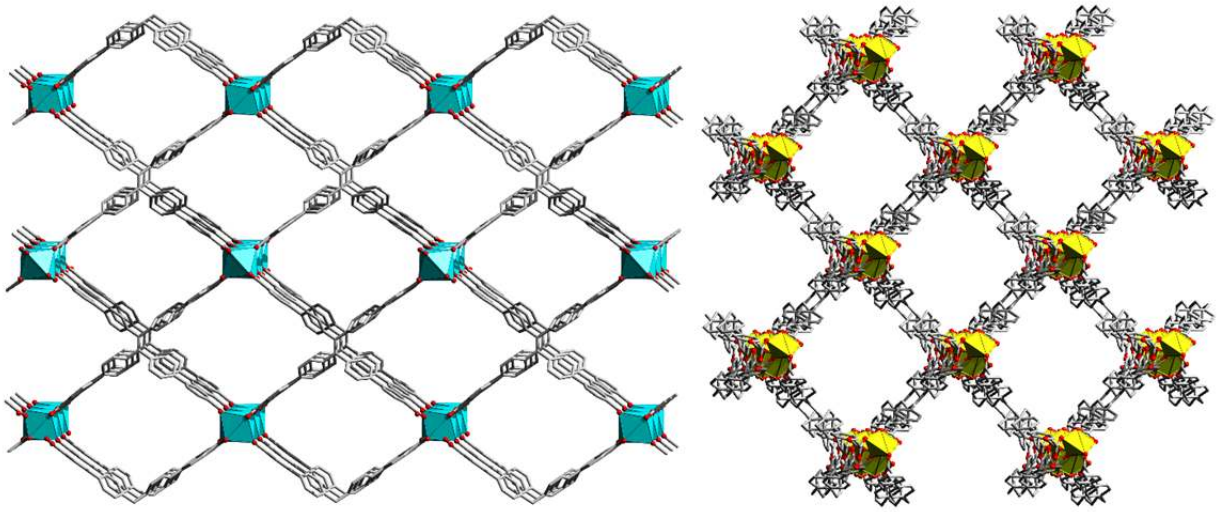

Figure 1 | Perspective view of In-MOF and Zn-MOF. Non-interpenetrated crystal structures of In-MOF (along *b*-axis) and Zn-MOF (along *c*-axis). C and O atoms are shown in grey and red. Coordination polyhedra of In and Zn atoms are represented in cyan and yellow. H atoms, DMA cations and interpenetrated networks are omitted for clarity. Please see Fig. S2 and S3 in the supporting information for the coordination at the metal nodes and perspective view along different directions.

The rigidification of highly fluorescent and otherwise conformationally flexible TCPE linkers between the metal nodes results in a great enhancement in the fluorescent properties with emission peaks at 494 nm upon excitation at 400 nm (Fig. 2b and S8 in SI), as compared to the parent, free acid H_4TCPE with emission at 534 nm. Inspired by this strong fluorescence behaviour, the material was subjected to a 100 fs laser at 800 nm. This laser is connected to an optical parametric amplifier (OPA) and coupled to a microscopic spectrometer in order to observe the anticipated nonlinear optical behaviour. Remarkably, the material showed very strong 2PEF with the emission maximum at 487 nm at λ_{ex} = 800 nm (Fig. S8 in SI). The 2PEF peak is slightly blue shifted by 7 nm compared to the 494 nm 1PEF due to reabsorption and other mechanisms.[24, 36, 37] The 2PEF has been quantified by comparing the emission data with a perylene reference sample at the same laser wavelength and power. The two-photon action cross section value of 3072 GM is much higher than the 55 GM of the free ligand (Fig. 3a and S5 in SI).[38, 39] The slope of the log-log dependence of the fluorescence intensity upon irradiation was found to be ~2 (power-dependent plots, Fig. S12 in SI), which confirms the third-order two-photon upconversion in the material. Similarly, wavelength-dependent 2PEF was measured to check for possible higher order nonlinearity. However, the compound did not show any higher-order nonlinear behaviour, which might be due to forbidden selection rules or very low activity at higher wavelengths and nonlinear orders.[40]

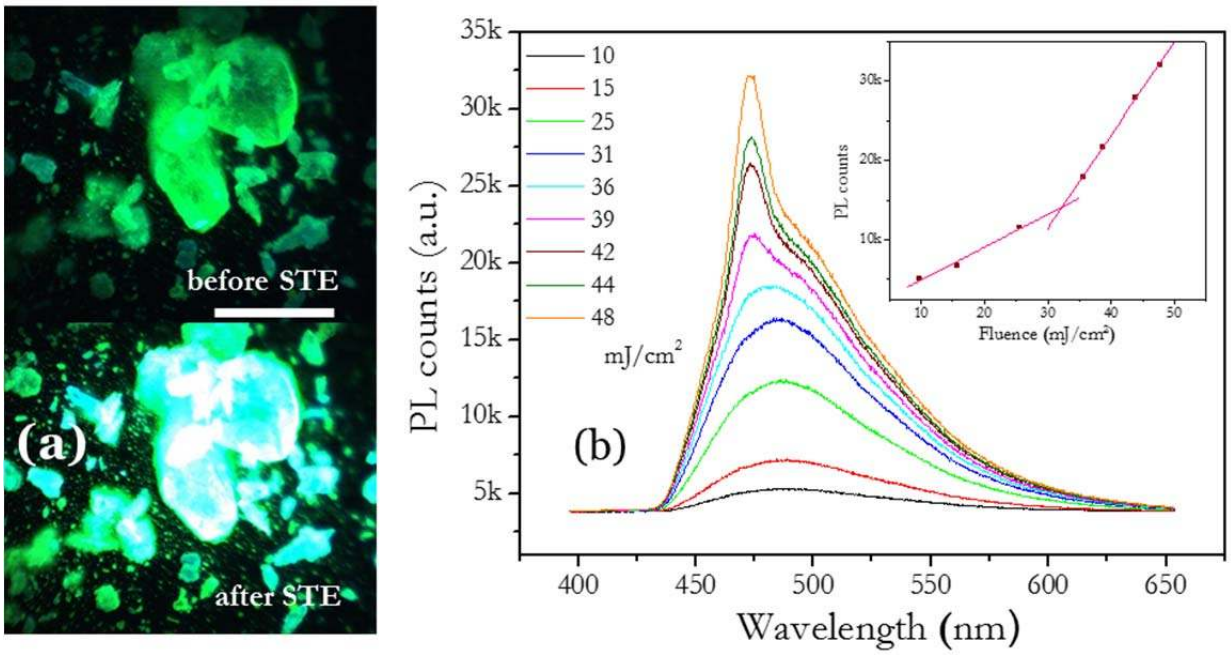

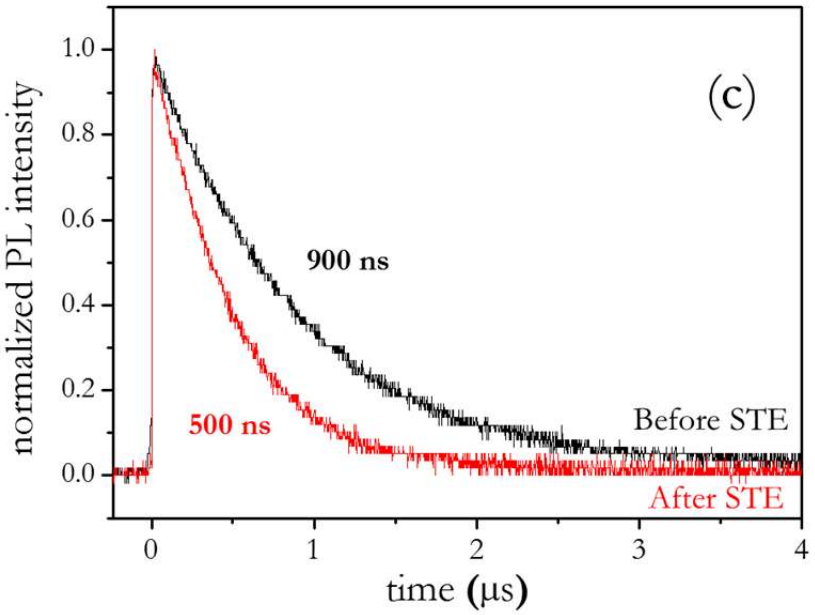

Figure 2 | Optical properties of In-MOF at different excitation laser power and its optical images upon excitation. a, optical images of In-MOF crystals below and above STE threshold; the scale bar is 100 μm; **b,** PL spectra at different laser powers at 400 nm excitation, change in slope of the fluorescence above STE threshold in In-MOFs (in set); **c,** photoluminescence decay curves below and above the STE threshold power and change in the fluorescence life times from 900 ns to 500 ns upon excitation at 400 nm.

During the power-dependent measurements at 400 nm excitation, a prominent sharp peak evolved from the fluorescence peak which emphasizes the possible stimulated emission from In-MOF (Fig. 2). We further analysed the fluorescence spectra (1PEF) and realized that the fluorescence peak can be deconvoluted into two Gaussian peaks (Fig. S6 in SI) with maxima at 482 nm and 522 nm and a FWHM of 84 nm and 50 nm, respectively (Fig. S6a & S6b in SI).

Upon increasing the power of the laser, a significant sharp peak at 472 nm with a FWHM of 18±2 nm evolved from the broad 1PEF (FWHM = 90 nm) fluorescence spectrum (Fig. S6c in SI). By plotting the power of the laser-dependent maximum intensity of the luminescence spectrum, the STE threshold was determined as 36 mJ/cm^2 (Fig. 2b). To further confirm the STE, time-resolved photoluminescence (TRPL) measurements were performed on these single crystals with laser powers below and above the STE threshold. These showed significant fluorescence life time decay from 900 ns to 500 ns. This suggests the faster recombination of exciton driven STE, which is consistent with the signature of stimulated emission as shown in Fig. 2c.[9, 11, 12]

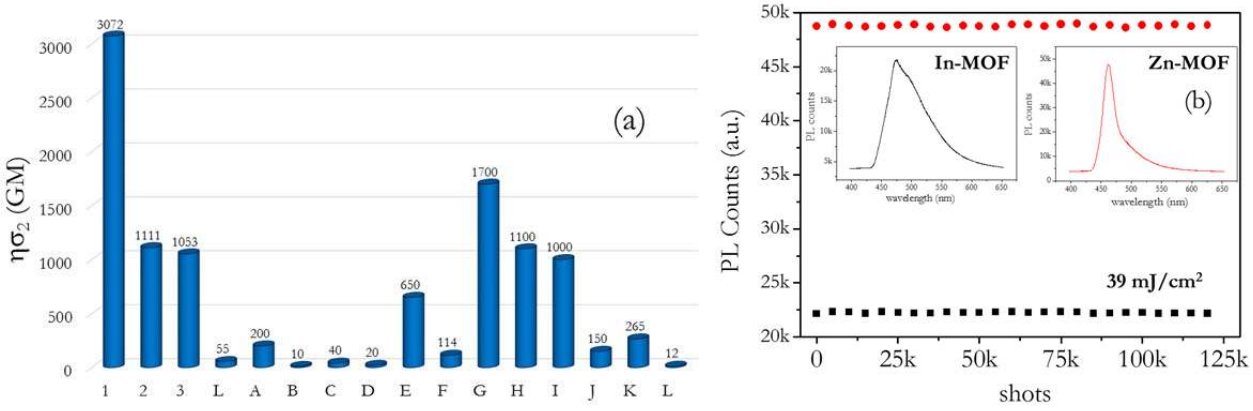

Figure 3 | Two photon excited PL/photo-upconversion of MOFs and its comparison with well-known materials and the optical stability of MOFs under laser. a, Comparison of 2PA cross section values of 1 (In-MOF), 2 (non-crystalline In-MOF), 3 (Zn-MOF), L (H_4TCPE), A (Rhodamine-B), B (Rhodamine-6G), C (Fluorescein), D (Coumarin 307), E (C18-RG), F (Porphyrin), G (Porph-20 layer film), H (Porph-50 layer film), I (CdSe QDs), J (CdTe QDs), K (Mn-doped-ZnS QDs) and L ([Zn_2(SDC)$_2$(An2Py)]·anthracene.[27-29, 38] **b,** Optical stability of In- (black squares) and Zn-MOF (red circles) at laser beam with pumping intensity of 39 mJ/cm^2. The fluorescence spectra during the measurement (in set).

A parallel or stacked arrangement of linkers should favour strong nonlinear 2PEF and spontaneous emission.[29] The low-density packing of the linkers could therefore be the reason for the relatively small stimulated peak of In-MOF. Hence, synthesis of related MOFs with denser packing was attempted for better population inversion and STE. In particular, Zn(II) was chosen as the node due to its relatively low coordination number (from 4 to 6), absence of d-d transitions (which might interfere with the optical properties) and its environmentally friendly behaviour. Yellow block-shaped single crystals of (DMA)[Zn(HTCPE)] (Zn-MOF; HTCPE = monoprotonated TCPE linker) were obtained by solvothermal synthesis employing $Zn(NO_3)_2$, H_4TCPE and 4,4′-bipyridylethelene in DMF/water/1M HCl solution at 110 °C. This Zn-MOF also crystallized in the monoclinic space group $P2_1/c$ and the structure was determined via single crystal X-ray diffraction measurements. The Zn(II) is coordinated to four carboxylates of TCPE in a distorted square pyramidal geometry. One carboxylate is coordinated in chelated manner, while the other three carboxylate groups are coordinated in monodentate fashion to Zn(II). This forms a 3D anionic framework (Fig. 1 and S3a in SI) with four-fold interpenetration and no

accessible porosity. One of the three monodentate carboxylates is protonated and the corresponding OH-group is hydrogen bonded to two neighbouring oxygen atoms of TCPE ligands. Overall, the Zn(II)-centres act as four connecting nodes by coordinating to four TCPE linkers. If the TCPE linkers are again considered as double tri-connected moieties, the topology of the framework is confirmed as another rare **dmd** net with stoichiometry $(3\text{-c})_2(4\text{-c})$ and point symbol $(4\cdot10^2)_2(4^2\cdot10^4)$. By further simplifying TCPE to four connected nodes the topology of the framework is confirmed as a **pts** net with stoichiometry (4-c)(4-c) and point symbol $(4^2\cdot8^4)$ (Fig. S4 in SI).[30, 31] Phase purity of Zn-MOF has also been confirmed by PXRD and a stability up to 400 °C was established by TGA (Fig. S10 and S15 in SI).

Nonlinear optical-absorption measurements were performed on Zn-MOF similar to In-MOF. These showed strong photo-upconversion with a 2PEF action cross-section value of 1053 GM at 650 nm. The mechanism of 2PEF has again been confirmed by power-dependent plots with slope ~2 (Fig. S12 in SI). The stronger 2PEF behaviour of In-MOF could be due to the different packing behaviour and conformation of the TCPE linkers.[29, 41] By careful analysis and comparison, the TCPE linkers turn out to be nicely arranged (superimposable position) along the *b*-axis in In-MOF (Fig. 1a) which causes the strong spontaneous emission with higher action cross-section values (Fig. S3 in SI).[29, 41] Power-dependent emission measurements have also been performed for Zn-MOF and revealed much better STE than for In-MOF with a sharp peak at 473 nm (FWHM =19±1 nm) away from the broad 1PEF spectrum (FWHM=70 nm) with lower threshold input laser fluence of 27 mJ/cm^2. The TRPL data show a decrease from 1.2 μs to 380 ns, which emphasizes the stimulated emission behaviour of Zn-MOF.[9, 11, 12] In addition, both materials (In-MOF and Zn-MOF) are very stable under laser illumination which has been confirmed by exposing them to optical pulses of 39 mJ/cm^2 for 1.25 x 10^5 pulses (Fig. 3b).

Unlike quantum dots, the STE peak is observed in the high energy region (blue side) of spontaneous emission. To understand such unique behaviour, the band structure along the high symmetry lines of the MOFs have been calculated by density-functional theory (DFT) (Fig S18 in SI). For the band structure calculations we used the all-electron code FHI-aims[42-44] and the dispersion-corrected generalized gradient functional PBE+vdW.[45, 46] At this level of theory, the band gap will be severely underestimated. When accounting for this by adjusting to the experimental optical gap, we find numerous valence bands in the energy range where STE is observed. A rationalization for the STE peak from the blue side of spontaneous emission could therefore be that the radiative decay of the STE occurs primarily from the higher excited state of conduction band to a lower level of valence band.

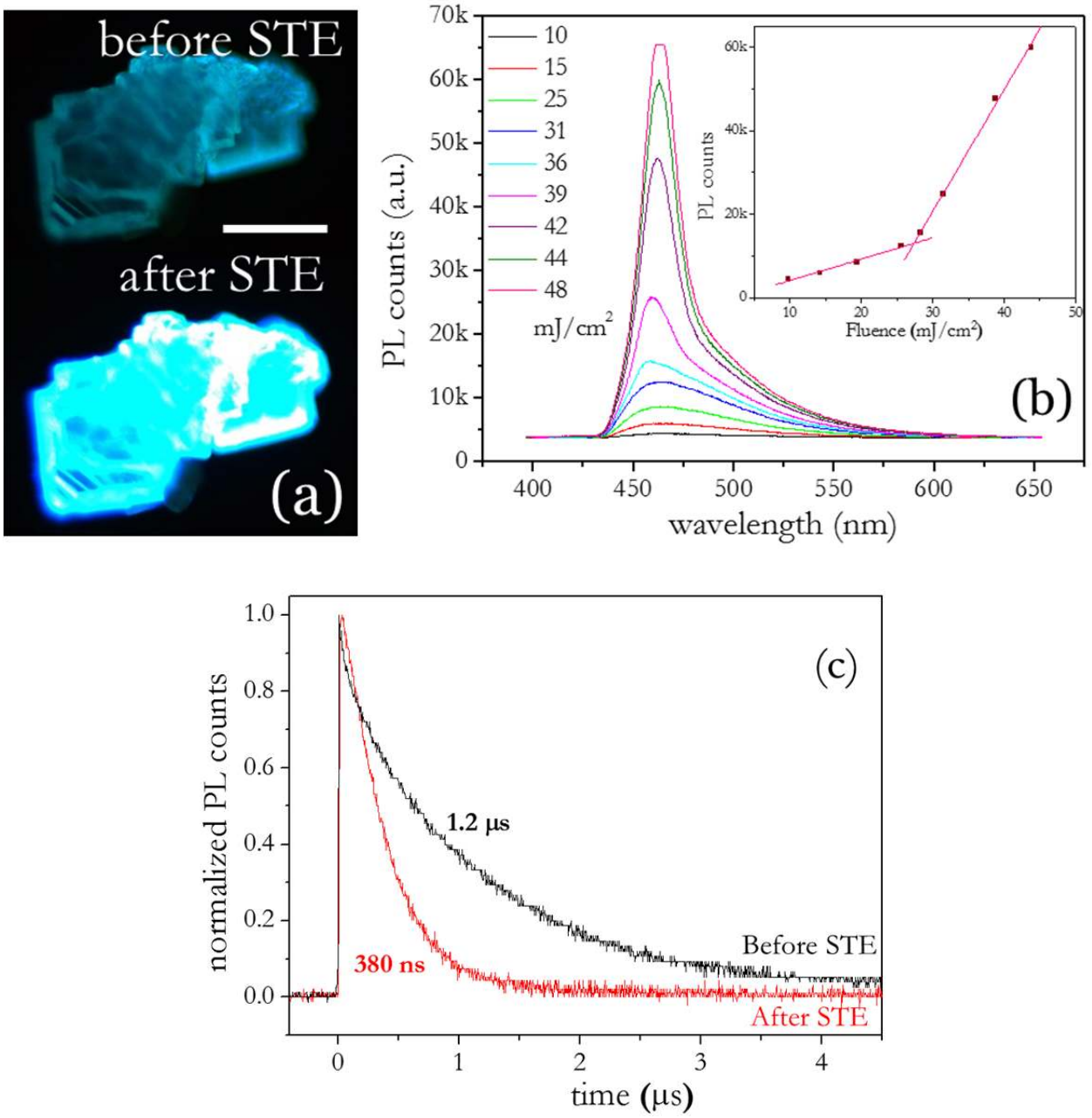

Figure 4 | Optical properties of Zn-MOF at different excitation laser power and its optical images upon excitation. a, optical images of Zn-MOF crystals below and above STE threshold; the scale bar is 100 μm. **b,** PL spectra at different laser powers at 400 nm excitation, change in slope of the fluorescence above STE threshold in In-MOFs (in set). **c,** Photoluminescence decay curves below and above the STE threshold power and change in the fluorescence life times from 1.2 μs to 380 ns upon excited by 400 nm.

Dye-loaded MOF composites were obtained to probe a further enhancement of the stimulated emission.[24-26] An attempt was made to exchange the DMA counterions of In-MOF and Zn-MOF with the cationic red dye molecule 4-[p-(dimethylamino)styryl]-1-methylpyridinium (DSMP). Partial exchange of the DMA cations in In-MOF was successful (~20% DMA exchange by DSMP according to spectroscopic data and elemental analysis), but

failed for Zn-MOF. This was expected from the very small channels and negligible porosity of Zn-MOF. Single-crystal measurements were performed to analyse the location of DSMP in the pores of In-MOF. However, localization of the dye was unsuccessful, which might be due to the incomplete cation exchange and a highly disordered arrangement of DSMP molecules in the pores (see SI). The optical characterization of this material showed strong quenching of fluorescence and NLO properties and no STE. This is assigned to the lack of proper arrangement of DSMP molecules to enhance the polarization in the material and thus more non-radiative decay takes place.[24-26] Stability of this composite material under laser showed significant photo-bleaching which can be easily identified by either shifting of the emission peak or decay in fluorescence intensity during our measurements (Fig. S18 in SI).

In conclusion, we have successfully achieved two anionic blue phosphor 3D interpenetrated MOFs with rare **tfi** and **dmd** connectivity. Upon excitation with femtosecond laser, these materials reveal unprecedented nonlinear optical properties and stimulated emission as intrinsic properties, which are controlled by the conformational and packing behaviour of the organic linkers that are pinned between the heavy metal-ion nodes of the framework. Exceptionally high nonlinear absorption with 2PEF action cross section values up to 3072 GM were found, highest for any hybrid solid state material. Our results not only reveal the unique optical properties, but also high photo- and thermal-stability of these materials. We envision that our concept and data will open-up coordination network materials, in particular MOFs, as a platform of solid-state dielectrics for producing novel nonlinear and optical gain materials, thereby offering the potential of surpassing conventional dyes in solution/liquid/fluid systems with limited practical applicability.

Acknowledgments:

R.M. would like to thank the Alexander von Humboldt Foundation for a post-doctoral fellowship. V.N. and H.S. would like to thank the Singapore Ministry of Education Academic Research Fund Tier 3 (Grant MOE2011-T3-1-005) for financial support. R.A.F would like to thank German Research Foundation for establishing Priority Program 1928 “Coordination Network Materials as Building Blocks for Functional Devices” (COORNETs).

Author contributions:

R.M., V.N., K.R. and R.A.F. conceived the idea. R.M. synthesised and characterized the compounds and V.N. performed the nonlinear optical studies, S.H. refined the single crystal structures and L.N. performed DFT calculations. R.M., N.V., R.A.F. wrote the manuscript with contributions from of all the authors.

Additional information

Supplementary information is available in the online version of the paper. Reprints and permissions information is available online at www.nature.com/reprints. Correspondence and requests for materials should be addressed to R.A.F.

Competing financial interests

The authors declare no competing financial interests.

References

1. Hill MT and Gather MC. Advances in small lasers. *Nature Photon.* **8,** 908-918 (2014).
2. Min W, Lu S, Chong S, Roy R, Holtom GR and Xie XS. Imaging chromophores with undetectable fluorescence by stimulated emission microscopy. *Nature* **461,** 1105-1109 (2009).
3. Dalton L. Nonlinear Optical Polymeric Materials: From Chromophore Design to Commercial Applications. In: Lee K-S (ed). *Polymers for Photonics Applications I*. Springer Berlin Heidelberg: Berlin, Heidelberg, 2002, pp 1-86.
4. Walker E and Rentzepis PM. Two-photon technology: A new dimension. *Nature Photon.* **2,** 406-408 (2008).
5. Günter P. Introduction. In: Günter P (ed). *Nonlinear Optical Effects and Materials*. Springer Berlin Heidelberg: Berlin, Heidelberg, 2000.
6. Zhang C, Zou C-L, Zhao Y, Dong C-H, Wei C, Wang H*, et al.* Organic printed photonics: From microring lasers to integrated circuits. *Sci. Adv.* **1,** (2015).
7. Zheludev NI, Prosvirnin SL, Papasimakis N and Fedotov VA. Lasing spaser. *Nature Photon.* **2,** 351-354 (2008).
8. Wang Y, Fong KE, Yang S, Ta Van D, Gao Y, Wang Z*, et al.* Unraveling the ultralow threshold stimulated emission from CdZnS/ZnS quantum dot and enabling high-Q microlasers. *Laser & Photonics Reviews* **9,** 507-516 (2015).
9. Zhu H, Fu Y, Meng F, Wu X, Gong Z, Ding Q*, et al.* Lead halide perovskite nanowire lasers with low lasing thresholds and high quality factors. *Nature Mater.* **14,** 636-642 (2015).
10. Lebeau B and Innocenzi P. Hybrid materials for optics and photonics. *Chem. Soc. Rev.* **40,** 886-906 (2011).
11. Wang Y, Li X, Zhao X, Xiao L, Zeng H and Sun H. Nonlinear Absorption and Low-Threshold Multiphoton Pumped Stimulated Emission from All-Inorganic Perovskite Nanocrystals. *Nano Letters* **16,** 448-453 (2016).
12. Wang Y, Li X, Song J, Xiao L, Zeng H and Sun H. All-Inorganic Colloidal Perovskite Quantum Dots: A New Class of Lasing Materials with Favorable Characteristics. *Adv. Mater.* **27,** 7101-7108 (2015).
13. Veldhuis SA, Boix PP, Yantara N, Li M, Sum TC, Mathews N*, et al.* Perovskite Materials for Light-Emitting Diodes and Lasers. *Adv. Mater.* **28,** 6804–6834 (2016).
14. Yong K-T, Law W-C, Hu R, Ye L, Liu L, Swihart MT*, et al.* Nanotoxicity assessment of quantum dots: from cellular to primate studies. *Chem. Soc. Rev.* **42,** 1236-1250 (2013).
15. Chuang C-HM, Brown PR, Bulović V and Bawendi MG. Improved performance and stability in quantum dot solar cells through band alignment engineering. *Nature Mater.* **13,** 796-801 (2014).
16. Huang S, Li Z, Kong L, Zhu N, Shan A and Li L. Enhancing the Stability of CH3NH3PbBr3 Quantum Dots by Embedding in Silica Spheres Derived from Tetramethyl Orthosilicate in "Waterless" Toluene. *J. Am. Chem. Soc.* **138,** 5749-5752 (2016).
17. Mei J, Leung NLC, Kwok RTK, Lam JWY and Tang BZ. Aggregation-Induced Emission: Together We Shine, United We Soar! *Chem. Rev.* **115,** 11718-11940 (2015).
18. Gong Q, Hu Z, Deibert BJ, Emge TJ, Teat SJ, Banerjee D*, et al.* Solution Processable MOF Yellow Phosphor with Exceptionally High Quantum Efficiency. *J. Am. Chem. Soc.* **136,** 16724-16727 (2014).
19. Shustova NB, Ong T-C, Cozzolino AF, Michaelis VK, Griffin RG and Dincă M. Phenyl Ring Dynamics in a Tetraphenylethylene-Bridged Metal–Organic Framework: Implications for the Mechanism of Aggregation-Induced Emission. *J. Am. Chem. Soc.* **134,** 15061-15070 (2012).
20. Wei Z, Gu Z-Y, Arvapally RK, Chen Y-P, McDougald RN, Ivy JF*, et al.* Rigidifying Fluorescent Linkers by Metal–Organic Framework Formation for Fluorescence Blue Shift and Quantum Yield Enhancement. *J. Am. Chem. Soc.* **136,** 8269-8276 (2014).
21. Cui Y, Li B, He H, Zhou W, Chen B and Qian G. Metal–Organic Frameworks as Platforms for Functional Materials. *Acc. Chem. Res.* **49,** 483-493 (2016).
22. Hu Z, Deibert BJ and Li J. Luminescent metal-organic frameworks for chemical sensing and explosive detection. *Chem. Soc. Rev.* **43,** 5815-5840 (2014).
23. Allendorf MD, Bauer CA, Bhakta RK and Houk RJT. Luminescent metal-organic frameworks. *Chem. Soc. Rev.* **38,** 1330-1352 (2009).

24. Yu J, Cui Y, Xu H, Yang Y, Wang Z, Chen B*, et al.* Confinement of pyridinium hemicyanine dye within an anionic metal-organic framework for two-photon-pumped lasing. *Nature Commun.* **4,** 2719 (2013).
25. Wei Y, Dong H, Wei C, Zhang W, Yan Y and Zhao YS. Wavelength-Tunable Microlasers Based on the Encapsulation of Organic Dye in Metal–Organic Frameworks. *Adv. Mater.***,** 10.1002/adma.201601844 (2016).
26. He H, Ma E, Cui Y, Yu J, Yang Y, Song T*, et al.* Polarized three-photon-pumped laser in a single MOF microcrystal. *Nature Commun.* **7,** 11087 (2016).
27. He GS, Tan L-S, Zheng Q and Prasad PN. Multiphoton Absorbing Materials: Molecular Designs, Characterizations, and Applications. *Chem. Rev.* **108,** 1245-1330 (2008).
28. Subha R, Nalla V, Yu JH, Jun SW, Shin K, Hyeon T*, et al.* Efficient Photoluminescence of Mn2+-Doped ZnS Quantum Dots Excited by Two-Photon Absorption in Near-Infrared Window II. *J. Phys. Chem. C* **117,** 20905-20911 (2013).
29. Collini E. Cooperative effects to enhance two-photon absorption efficiency: intra- versus inter-molecular approach. *Phys. Chem. Chem. Phys.* **14,** 3725-3736 (2012).
30. Li M, Li D, O'Keeffe M and Yaghi OM. Topological Analysis of Metal–Organic Frameworks with Polytopic Linkers and/or Multiple Building Units and the Minimal Transitivity Principle. *Chem. Rev.* **114,** 1343-1370 (2014).
31. Blatov VA, Shevchenko AP and Proserpio DM. Applied Topological Analysis of Crystal Structures with the Program Package ToposPro. *Cryst. Growth Des.* **14,** 3576-3586 (2014).
32. Baxter EF, Bennett TD, Cairns AB, Brownbill NJ, Goodwin AL, Keen DA*, et al.* A comparison of the amorphization of zeolitic imidazolate frameworks (ZIFs) and aluminosilicate zeolites by ball-milling. *Dalton Trans.* **45,** 4258-4268 (2016).
33. Henke S, Schmid R, Grunwaldt J-D and Fischer RA. Flexibility and Sorption Selectivity in Rigid Metal–Organic Frameworks: The Impact of Ether-Functionalised Linkers. *Chem. Eur. J.* **16,** 14296-14306 (2010).
34. Chapman KW, Halder GJ and Chupas PJ. Pressure-Induced Amorphization and Porosity Modification in a Metal−Organic Framework. *J. Am. Chem. Soc.* **131,** 17546-17547 (2009).
35. Bennett TD, Tan J-C, Yue Y, Baxter E, Ducati C, Terrill NJ*, et al.* Hybrid glasses from strong and fragile metal-organic framework liquids. *Nature Communications* **6,** 8079 (2015).
36. Wang Y, Ta VD, Gao Y, He TC, Chen R, Mutlugun E*, et al.* Stimulated Emission and Lasing from CdSe/CdS/ZnS Core-Multi-Shell Quantum Dots by Simultaneous Three-Photon Absorption. *Adv. Mater.* **26,** 2954-2961 (2014).
37. He T, Rajwar D, Ma L, Wang Y, Bang Lim Z, Grimsdale AC*, et al.* Wavelength dependence of optical nonlinearity of terpyridine-based Zn(II)-coordinated rigid linear polymers. *Appl. Phys. Lett.* **101,** 213302 (2012).
38. Quah HS, Chen W, Schreyer MK, Yang H, Wong MW, Ji W*, et al.* Multiphoton harvesting metal-organic frameworks. *Nature Commun.* **6,** 7954 (2015).
39. Makarov NS, Drobizhev M and Rebane A. Two-photon absorption standards in the 550-1600 nm excitation wavelength range. *Opt. Express* **16,** 4029-4047 (2008).
40. Masters BR and So P. *Handbook of Biomedical Nonlinear Optical Microscopy*. Oxford University Press, 2008.
41. Medishetty R, Nemec L, Nalla V, Henke S, Zheludev N, Samoć M*, et al.* Multi-Photon Absorption in MOFs Controlled by Charge Polarization, Conformational Strain and Alignment. *submitted***,**
42. Havu V, Blum V, Havu P and Scheffler M. Efficient integration for all-electron electronic structure calculation using numeric basis functions. *J. Comput. Phys.* **228,** 8367-8379 (2009).
43. Blum V, Gehrke R, Hanke F, Havu P, Havu V, Ren X*, et al.* Ab initio molecular simulations with numeric atom-centered orbitals. *Comput. Phys. Commun.* **180,** 2175-2196 (2009).
44. Auckenthaler T, Blum V, Bungartz HJ, Huckle T, Johanni R, Krämer L*, et al.* Parallel solution of partial symmetric eigenvalue problems from electronic structure calculations. *Parallel Computing* **37,** 783-794 (2011).
45. Perdew JP, Burke K and Ernzerhof M. Generalized Gradient Approximation Made Simple. *Phys. Rev. Lett.* **77,** 3865-3868 (1996).
46. Tkatchenko A and Scheffler M. Accurate Molecular Van Der Waals Interactions from Ground-State Electron Density and Free-Atom Reference Data. *Phys. Rev. Lett.* **102,** 073005 (2009).

377

Methods

In-MOF: A mixture of $InCl_3$ (4 mg, 0.018 mmol), H_4TCPE (8 mg, 0.009 mmol) were dissolved in *N,N*-dimethylformamide (DMF, 2 mL), ethanol (0.5 ml) and 10 µl 1M HCl in 4 ml glass vial. This reaction mixture was placed in programmable oven and heated at 85 °C for 48 h followed by cooling to room temperature at the rate of 5 °C·h^{-1}. Pale yellow block shaped single crystals of In-MOF, [In(TCPE)](DMA) were obtained and these crystals were washed with excess DMF, ethanol and dried at room temperature. Yield: 8 mg, 73%, Anal. Calcd (%): C, 69.36; H, 4.16; N, 1.44. Found: C, 69.65; H, 3.96; N, 1.60. (Porous crystalline materials, MOFs are known to trap guest molecules, hence, it is difficult to fit the EA data. So we provided the calculated elemental content based on the chemical formula of activated sample.)

Zn-MOF: A mixture of $Zn(NO_3)_2{\cdot}4H_2O$ (14 mg, 0.054 mmol), H_4TCPE (8 mg, 0.009 mmol) and 4,4'-bipyridylethene (3 mg, 0.017 mmol) were dissolved in DMF (2 mL), methanol (0.5 ml) and 10 µl 1M HCl in 4 ml glass vial and placed in programmable oven and heated to 110 °C for 48 h followed by cooling to room temperature at the rate of 5 °C·h^{-1}. Pale yellow rod like single crystals of Zn-MOF, [Zn(HTCPE)](DMA) were obtained. These crystals were washed with excess DMF, methanol and dried at room temperature. Yield: 7.5 mg, 81%, Anal. Calcd (%): C, 73.00; H, 4.49; N, 1.52. Found: C, 72.56; H, 4.25; N, 1.65.

Dye loading in In-MOF: The In-MOF single crystals were placed in dil. DSMP solution in DMF and the solvent was exchanged for every 8 h with slight increment of the dye concentration from 0.25 mM to 12 mM for 4 days. The elemental analysis of activated sample shows almost 20 % exchange of DMA cation with DSMP. Anal. Calcd (%): C, 70.04; H, 4.22; N, 1.67. Found: C, 70.14; H, 4.35; N, 1.85.

Loading of Rh-B in In-MOF has been attempted but it was not so successful due to neutral state of Rh-B compound. It might be due to the basicity of the MOF system, the colour of the Rh-B in DMF has been vanished while soaking the In-MOF single crystals in Rh-B solution. After several cycles of solvent exchange for more than a week, the colour of the single crystals was changed to pale pink, but the pink colour completely vanished under the laser and the crystals returned to yellow. This might be due to the decay of the dye in the pores of MOF.

Two-photon excited PL and STE: TPEF and STE of MOF crystals were measured with 100-fs laser pulses (580–1000 nm wavelength and 1 kHz repetition rate) emitted from a mode locked Ti: sapphire laser (Spectra Physics, Maitai-Spitfire) pumped OPA. Single crystal MOF samples were kept on a glass plate; this glass plate was mounted on microscope stage. The laser pulses were focused onto the sample with a 10X microscope objective (NA=0.3). Optical density filters were used to change incident laser energy. The PL signal was collected using same microscope objective in reflection mode and dispersed by a monochromator (Princeton Instruments, Isoplane) and the spectrum was recorded by a charged coupled device (CCD, Andor). During the measurement, a dichroic filter was used to block the pump beam. Transient PL signals were collected using fast photo-diode (Rise time ~ 1 ns), signals are coupled in to the digital oscilloscope.

DFT calculations: The band structures are obtained by numerically and basis-set converged DFT calculations using the FHI-aims all-electron code together with the dispersion-corrected generalized-gradient PBE+vdW functional. Brillouin-zone sampling was done on a 2x2x2 integration grid, with the final band structure plotted along densely sampled high-symmetry lines. The crystallographic data for the In- and Zn-MOFs were used as input structures for our calculations.